Influence of Thermal Treatments, Molecular Weight, and Molecular Weight Distribution on the Crystallization of β-Isotactic Polypropylene

Antonio Marigo,[1] Carla Marega,[1] Valerio Causin,[1] Paolo Ferrari[2]

[1]*Dipartimento di Chimica Inorganica, Metallorganica ed Analitica dell'Università, via Loredan, 4, 35131 Padova, Italy*
[2]*Basell Poliolefine Italia SpA — Centro Ricerche "G. Natta", P.le Donegani 12, 44100 Ferrara, Italy*

Received 5 April 2003; accepted 13 June 2003

ABSTRACT: Six samples of isotactic polypropylene were examined to study the influence of the thermal treatments and the molecular weights and their distribution on the β-crystallization of the polymer. The highest amount of the β-phase was obtained by isothermal crystallization and in correspondence of high average molecular weights and wide molecular weight distributions. Small-angle X-ray scattering pointed out that a partial β-crystallization seems not to influence the lamellar morphology parameters. Differential scanning calorimetry measurements, at different heating rates, allowed us to confirm that the multiple melting endotherms behavior of the β-phase is to be correlated to a melting–recrystallization–melting mechanism. © 2003 Wiley Periodicals, Inc. J Appl Polym Sci 91: 1008–1012, 2004

Key words: isotactic polypropylene; β-crystallization; DSC; WAXS; SAXS

INTRODUCTION

The hexagonal β-form of isotactic polypropylene (iPP) was identified by Keith et al.[1] in 1959. It crystallizes from the melt with the aid of nucleating agents,[2–5] or by rapid quench from the melt to below 130°C,[6] or, again, from melts subjected to shear.[7,8] The β-iPP form usually crystallizes together with the other crystalline phases of iPP[6] and it often exhibits, similar to the α-phase,[9] two melting endotherms in differential scanning calorimetry (DSC).[10,11]

Furthermore, the β-form is metastable with respect to the monoclinic α-form,[12–14] then it tends to converts to the α-form when the sample is subjected to appropriate thermal treatment.[15–17] DSC and wide-angle X-ray scattering (WAXS) measurements pointed out that the β–α transition during heating essentially consists of the melting of the β-form and the successive recrystallization in the α-form.[15–17]

This article is concerned with the influence of thermal treatments on β-crystallization and lamellar morphology of iPP samples with different average molecular weights and molecular weights distributions. The crystallization was induced by quenching from the melt and by isothermal treatments at different temperatures. The total degree of crystallinity and the relative amounts of β-form were evaluated by WAXS, whereas the small-angle X-ray scattering (SAXS) technique gave the parameters of the lamellar stackings, as the average thicknesses of the crystalline lamellae and of the amorphous regions and their distributions. Furthermore, DSC measurements were performed, at different heating rates, to confirm the melting–recrystallization–melting mechanism of the β–α transition.

Correspondence to: A. Marigo (antonio.marigo@unipd.it).

Journal of Applied Polymer Science, Vol. 91, 1008–1012 (2004)

EXPERIMENTAL

Materials

Six iPP samples, supplied by Basell Poliolefine SpA (Ferrara, Italy), were used in this study and Table I reports the data of viscosity average molecular weights, $\overline{M}_v$, and molecular weight polydispersity index (PI), which was obtained by rheological measurements.[18] All the samples were comparable as concerns the Isotacticity Index (II ≈ 98%, determined by the insoluble xylene).

The samples were achieved via liquid propylene polymerization by using standard high-yield Ziegler–Natta catalysts; broad molecular weight distribution products were obtained via sequential bimodal polymerization. After polymerization, the spherical form iPP products were pelletized with a Berstoff ZE25 twin-screw extruder, adding conventional thermal and processing stabilizers; no nucleating agents were added.

The pellets were then transformed into plaques by compression molding in a press at 200°C for 10 min and cooled by water/ice quenching or by isothermically crystallization by a rapid transfer of the samples

TABLE I
Viscosity Average Molecular Weights $\overline{M}_v$ and Molecular Weight Polydispersity Index PI of the iPP Samples

Samples	$\overline{M}_v$	PI
P1	2.14×10^5	4.0
P2	2.18×10^5	8.4
P3	2.09×10^5	10.2
P4	3.55×10^5	4.0
P5	3.78×10^5	7.0
P6	3.78×10^5	7.6

from the press into an oven at the selected crystallization temperature T_c (±0.4°C) followed, after 3 h, by water/ice quenching.

Differential scanning calorimetry

All the measurements were carried out with a TA Instruments model 2920 calorimeter operating under nitrogen atmosphere. Indium of high purity was used for calibrating the DSC temperature and enthalpy scales.

Wide-angle X-ray scattering

The WAXS patterns of the samples were recorded in the diffraction angular range of 10–30° 2θ by a transmission diffractometer GD 2000 produced by Ital Structures (Riva del Garda, Italy), working in the Seemann–Bohlin geometry and with a quartz crystal monochromator of the Johansson type on the primary X-ray beam; Cu$K_{\alpha 1}$ radiation was employed. The application of the least-squares fit procedure elaborated by Hindeleh and Johnson[19] gave the total degree of crystallinity (ϕ_{tot}). The relative content of β-form was determined by[6]:

$$\phi_\beta = \frac{A(300)}{A(300) + A(110) + A(040) + A(130)} \quad (1)$$

where $A(110)$, $A(040)$, and $A(130)$ are the areas under the three equatorial α-form peaks (110), (040), and (130), while $A(300)$ is the area under the β-form peak (300). The areas were determined by the fitting procedure described above.

Small-angle X-ray scattering

The SAXS patterns of the samples were recorded by a MBraun system, utilizing the Cu$K\alpha$ radiation from a Philips PW 1830 X-ray generator. The data were collected by a position-sensitive detector, in the scattering angular range of 0.1–5.0° (2θ) and were successively corrected for the blank scattering.

A constant continuous background scattering was then subtracted[20] and the obtained intensity values $\tilde{I}(s)$ were smoothed in the tail region, with the aid of the $s\tilde{I}(s)$ versus $1/s^2$ plot.[21] Finally, the Vonk's desmearing procedure[22] was applied and the one-dimensional scattering function was obtained by the Lorentz correction $I_1(s) = 4\pi s^2 I(s)$, where $I_1(s)$ is the one-dimensional scattering function and $I(s)$ is the desmeared intensity function, being $s = (2/\lambda)\sin\theta$.

SAXS data analysis

The evaluation of the SAXS patterns according to some theoretical distribution models[23,24] was carried out referring to the Hosemann model,[25] that assumes the presence of lamellar stacks having an infinite side dimension. This assumption, in practice, takes into account a monodimensional electron density change along the normal direction to the lamellae. According to this model, the intensity profile is evaluated as:

$$I(s) = I'(s) + I''(s) \quad (2)$$

where

$$I'(s) = \frac{(\rho_c - \rho_a)^2}{4\pi^2 s^2 D} \frac{|1 - F_C|^2(1 - |F_A|^2) + |1 - F_A|^2(1 - |F_C|^2)}{|1 - F_C F_A|^2} \quad (3)$$

$$I''(s) = \frac{(\rho_c - \rho_a)^2}{2\pi^2 s^2 DN} \mathrm{Re}\left\{\frac{F_A(1 - F_C)^2[1 - (F_A F_C)^N]}{(1 - F_A F_C)^2}\right\} \quad (4)$$

In these equations, F_C and F_A represent the Fourier transforms of the distribution functions of the lamellar thicknesses C and of the amorphous regions A, and ρ_c and ρ_a are the electron densities of the crystalline and amorphous regions, respectively, N is the number of the lamellae in the stack, and D is the average long period. A fitting procedure of the calculated one-dimensional scattering functions with the experimental procedures allows us to optimize the values of the crystalline and amorphous region thicknesses.

RESULTS AND DISCUSSION

WAXS analysis

The WAXS analysis of the quenched samples pointed out the presence of the β-phase only in samples P5 and P6, which gave a relative content ϕ_β equal to 0.04 and 0.08, respectively. These two samples were isothermally crystallized at T_c = 90°, 110°, and 140°C to get the best conditions to induce the crystallization in β-form.

Figure 1 shows the WAXS patterns of the isothermally crystallized sample P6 and it can be noted that

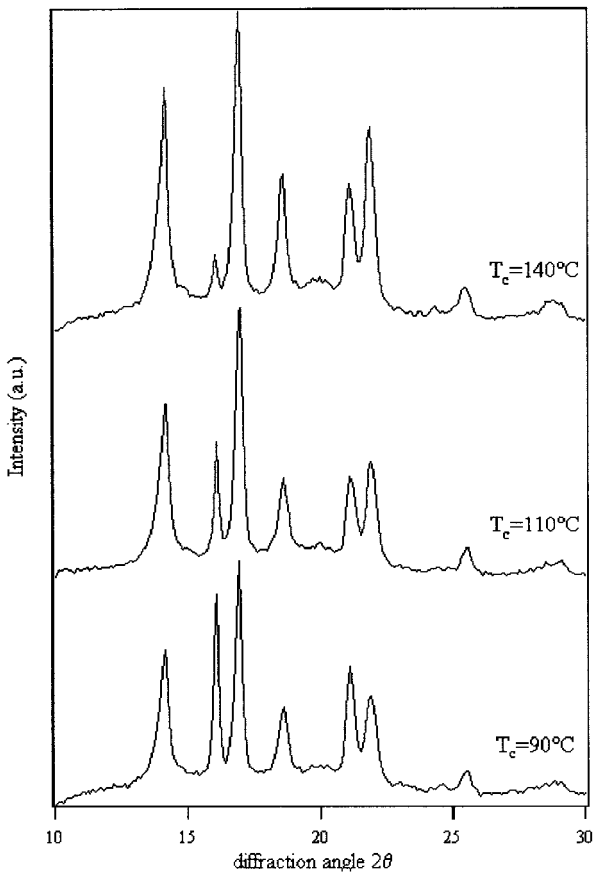

Figure 1 WAXS patterns of the sample P6 at different crystallization temperatures.

the intensity of the β-phase diffraction peak 300 at 16° 2θ increases with the lowering of T_c. As a matter of fact, the data of Table II demonstrate that the thermal treatments, which more greatly induces the crystallization in β-form of the samples P5 and P6, is the isothermal crystallization at 90°C.

On the basis of these results, all the samples were isothermally crystallized at 90°C and Table III reports the ϕ_{tot} and ϕ_β values, which were obtained from the WAXS patterns. The total degree of crystallinity does not show a particular trend with the molecular weight and its distribution, but the behavior of the samples as concerns the crystallization in β-form is interesting.

First of all, it is useful to compare the samples, P1,2,3, which have comparable and low molecular weights and growing polydispersity index from P1 to P3; the relative contents of β-form are low, independent of the PI index.

TABLE III
Total Degree of Crystallinity ϕ_{tot} and Relative Content of the β-Form ϕ_β in the iPP Samples, Isothermally Crystallized at T_c = 90°C

Samples	ϕ_{tot}	ϕ_β
P1	0.74	0.02
P2	0.63	0.01
P3	0.70	0.03
P4	0.75	=
P5	0.74	0.07
P6	0.78	0.19

As concerns the samples, P4,5,6, which have higher molecular weights than P1,2,3 and increasing PI index from P4 to P6, it can be noted that sample P4 wholly crystallizes in α-form, while the samples P5 and P6 have higher ϕ_β values than samples P1,2,3. In particular, the sample P6 gives the highest relative content of β-phase (ϕ_β = 0.19) among the examined samples. Then, the β-crystallization seems to be induced by the high molecular weights, but this condition is not enough, as the result of sample P4 demonstrates. The WAXS analysis points out that the concurrence of two factors is needed: high molecular weight and a wide distribution of molecular weights. This is confirmed by the behavior of the sample P6, which has practically the same average molecular weight than P5, but a wider distribution of molecular weight, and gives the highest fraction of β-form.

SAXS analysis

The isothermally crystallized samples were also analyzed by SAXS. The best fits between calculated and experimental patterns were achieved with Gaussian distribution functions of the lamellar and amorphous layers thicknesses. Figure 2 shows the fit of sample P6 and Table IV reports the lamellar morphology parameters of all the samples, as obtained by the analysis of the SAXS patterns.

The SAXS data do not show substantial differences among the samples, apart from a slight increase of the lamellar thickness in the sample P6; however, the

TABLE II
Total Degree of Crystallinity ϕ_{tot} and Relative Content of the β-Form ϕ_β in the Samples P5 and P6, Isothermally Crystallized at T_c

	T_c = 90°C		T_c = 110°C		T_c = 140°C	
Samples	ϕ_{tot}	ϕ_β	ϕ_{tot}	ϕ_β	ϕ_{tot}	ϕ_β
P5	0.74	0.07	0.75	0.03	0.78	=
P6	0.78	0.19	0.77	0.11	0.81	0.04

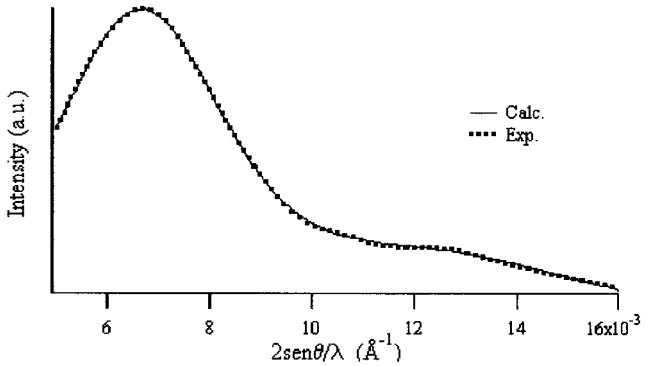

Figure 2 SAXS pattern of the sample P6 crystallized at T_c = 90°C.

presence of a nonnegligible fraction of β-form, as in sample P5 and P6, seems not to influence the parameters of the lamellar morphology. This result differs from that obtained from the analysis of the SAXS profiles of iPP samples, which crystallize in both α- and γ-form,[26] because, in that case, when the two phases were present in comparable fractions, it was necessary to use a bimodal distribution function of the thicknesses. However the β-form fraction of the samples P5 and P6 are lower with respect to the γ-form fraction of the samples examined in ref. 25.

DSC analysis

DSC heating scans were performed on the isothermally crystallized sample P6, which contains the highest fraction of β-form, to confirm the mechanism of melting–recrystallization–melting, which is held responsible for the multiple endotherms behavior of that iPP form.

The DSC scans were accomplished at different heating rates (1, 5, and 10°C/min) and the results are reported in Figure 3. There are always at least three melting endotherms at 150, 155, and 165°C, while the scan at 1°C/min shows also a fourth endotherm at 169°C.

Fujiwara[10] and Shi et al.[17] demonstrated that the first two peaks (150 and 155°C) are to be ascribed to the melting of the original β_1-form followed by recrystallization, during the temperature scanning, in a more stable β_2-form and by its melting. Furthermore, the third endotherm (165°C) is connected with the melting of the original α crystals and of those recrystallized after the melting of β_2.

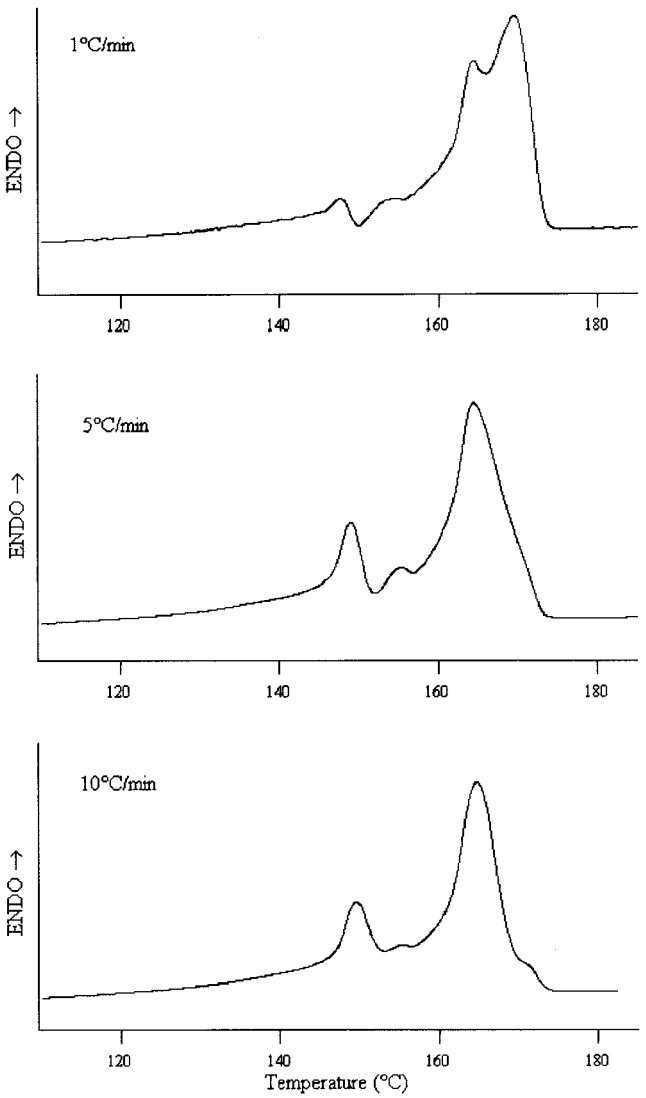

Figure 3 DSC patterns at different heating rates of the sample P6 crystallized at T_c = 90°C.

The DSC scans of Figure 3 confirm this mechanism; when the heating rate was low (1°C/min), a slight

TABLE IV
Lamellar (C) and Amorphous Phases (A) Average Thicknesses, Long Period (D), and Thickness Distribution Values (σ_C/C, σ_A/A, and σ_D/D) of the iPP Samples, Crystallized at T_c = 90°C

Samples	C (Å)	A (Å)	D (Å)	σ_C/C	σ_A/A	σ_D/D
P1	110	35	145	0.14	0.14	0.11
P2	111	35	146	0.15	0.15	0.12
P3	111	33	144	0.16	0.16	0.13
P4	106	37	143	0.19	0.19	0.15
P5	110	36	146	0.17	0.18	0.14
P6	118	38	156	0.13	0.13	0.11

exotherm peak points out the recrystallization of the more stable β_2-form, after the melting of β_1. When the heating rate increases (5 and 10°C/min), the melting peak of β_1 becomes more intense with respect to the second endotherm, which is to be ascribed to the melting of β_2, and the exotherm peak intensity lowers so much that it becomes undetectable.

Evidently, the amount of the recrystallization β_1–β_2 decreases with the increase of the heating rate. In a similar way, the intensity of the β-melting endotherms increases, with respect to the α-melting endotherms, when the heating rate increases. Then, the endotherm at higher temperatures are to be ascribed to the melting of the original and of the recrystallized α-form. When the heating rate is low (1°C/min), the double melting behavior of iPP-α can be noted, as already described in the literature.[9]

CONCLUSIONS

Some interesting remarks can be emphasized after this study on the β-crystallization of iPP, without the aid of the nucleating agent; as follows. (1) The highest relative content of β-form was achieved after an isothermal crystallization at 90°C and this condition gives better results than the quenching from the melt. (2) The driving force of the β-crystallization seems to be the concurrence of high molecular weights and of a wide distribution of molecular weights, together with a suitable thermal treating. (3) The presence of an nonnegligible fraction of β-form, together with the α-form, seems not to influence the parameters of the lamellar morphology, neither as concerns the average thicknesses of the lamellar and amorphous layers nor the distribution of these parameters. (4) It was confirmed that the multiple melting endotherms behavior of iPP samples containing both α and β forms is to be ascribed to the melting–recrystallization–melting of β_1 and β_2 forms, followed by the melting the original α crystals and of those recrystallized after the melting of β_2.

References

1. Keith, H. D.; Padden, F. J., Jr.; Walter, N. M.; Wyckoff, H. W. J Appl Phys 1959, 30, 1485.
2. Binsbergen, F. L.; de Lange, B. G. M. Polymer 1968, 9, 23.
3. Filho, D. S.; Oliveira, C. M. F. Makromol Chem 1993, 194, 279.
4. Garbarczyk, J.; Sterzynski, T.; Paukszta, D. Polym Commun 1989, 30, 153.
5. Kotek, J.; Raab, M.; Baldrian, J.; Grellmann, W. J Appl Polym Sci 2002, 85, 1174.
6. Turner Jones, A.; Aizlewood, J. M.; Beckett, D. R. Makromol Chem 1964, 75, 134.
7. Dragaun, H.; Hubeny, H. J Polym Sci Polym Phys Ed 1977, 15, 1779.
8. Moitzi, J.; Skalicky, P. Polymer 1993, 34, 3168.
9. Guerra, G.; Petraccone, V.; Corradini, P.; De Rose, C.; Napolitano, R.; Pirozzi, B.; Giunchi, G. J Polym Sci, Polym Phys Ed 1984, 22, 1029.
10. Fujiwara, Y. Colloid Polym Sci 1975, 253, 273.
11. Shi, G.; Cao, Y.; Huang, B.; Huang, S. Acta Polym Sin, 1987, 359.
12. Padden, F. J.; Keith, H. D. J Appl Phys 1959, 30, 1479.
13. Varga, J. J Mater Sci 1992, 27, 2557.
14. Morrow, D. R. J Macromol Sci Phys 1969, 3(B), 53.
15. Zhou, G.; He, Z.; Yu, J.; Han, Z.; Shi, G. Makromol Chem 1986, 187, 633.
16. Shi, G.; Huang, B.; Cao, Y.; He, Z.; Han, Z. Makromol Chem 1986, 187, 643.
17. Shi, G.; Zhang, X.; Cao, Y.; Hong, J. Makromol Chem 1993, 194, 269.
18. Morini, G.; Pennini, G.; Albizzati, E.; Ju Yoo, H. Pat. (Himont Inc.) Eur. Pat. 622, 380 A1.
19. Hindeleh, A. M.; Johnson, D. J. J Phys D: Appl Phys 1971, 4, 259.
20. Vonk, C. G.; Pijpers, A. P. J Polym Sci, Part B: Polym Phys 1985, 23, 2517.
21. Vonk, C. G. J Appl Crystallogr 1973, 6, 81.
22. Vonk, C. G. J Appl Crystallogr 1971, 4, 340.
23. Blundell, D. J. Polymer 1978, 18, 1343.
24. Marega, C.; Marigo, A.; Cingano, G.; Zannetti, R.; Paganetto, G. Polymer 1996, 37, 5549.
25. Hosemann, R.; Bagchi, S. N. Direct Analysis of Diffraction by Matter; North-Holland; Amsterdam, 1962.
26. Marigo, A.; Marega, C.; Saini, R.; Camurati, I. J Appl Polym Sci 2001, 79, 375.